

Graph Contrastive Learning with Implicit Augmentations

Huidong Liang^{a,b,1,2,*}, Xingjian Du^{b,1}, Bilei Zhu^b, Zejun Ma^b, Ke Chen^c, Junbin Gao^a

^a*Discipline of Business Analytics, The University of Sydney Business School, The University of Sydney, Australia*

^b*ByteDance AI Lab, Shanghai, China*

^c*University of California San Diego, San Diego, United States*

Abstract

Existing graph contrastive learning methods rely on augmentation techniques based on random perturbations (e.g., randomly adding or dropping edges and nodes). Nevertheless, altering certain edges or nodes can unexpectedly change the graph characteristics, and choosing the optimal perturbing ratio for each dataset requires onerous manual tuning. In this paper, we introduce *Implicit Graph Contrastive Learning* (iGCL), which utilizes augmentations in the latent space learned from a Variational Graph Auto-Encoder by reconstructing graph topological structure. Importantly, instead of explicitly sampling augmentations from latent distributions, we further propose an upper bound for the expected contrastive loss to improve the efficiency of our learning algorithm. Thus, graph semantics can be preserved within the augmentations in an intelligent way without arbitrary manual design or prior human knowledge. Experimental results on both graph-level and node-level tasks show that the proposed method achieves state-of-the-art performance compared to other benchmarks, where ablation studies in the end demonstrate the effectiveness of modules in iGCL.

Keywords: graph neural networks, contrastive learning, latent augmentations, graph auto-encoders

2010 MSC: 00-01, 99-00

1. Introduction

Graph Neural Networks (GNN) and their variants [1, 2, 3, 4] have achieved state-of-the-art performance on both graph-level and node-level tasks such as social network analysis [5], molecular interactions [6] and recommender systems [7]. In many scenarios, training end-to-end GNN models with supervision is impractical as label information is frequently unavailable or difficult to retrieve. Meanwhile, Self-Supervised Learning (SSL), an unsupervised method that first trains model on auxiliary tasks without label information and then uses the learned embeddings for downstream tasks, has gradually gained popularity in recent literature [8]. As one

of the effective pre-training designs, Graph Contrastive Learning (GCL), which aims to maximize the mutual information of the inputs and their counterparts, becomes a current representative of graph SSL method [9].

To generate different views (augmentations) for the input graphs, existing GCL methods at both node-level [10, 11, 12] and graph-level [13, 14, 15] rely on augmentations based on random perturbations, including randomly adding or dropping the graph's edges or nodes, and shuffling or masking node attributes. These augmentation approaches are based on a strong assumption that a small random perturbation will not alter the semantic property of the original graph [13]. Nevertheless, this assumption involves two critical issues. First, manipulations of edges and nodes on graphs in specific domains can ruin the data. For example, removing or appending certain edges or nodes in a molecular graph or a knowledge graph may immediately destruct the fundamental properties of graph [16], hence leading to fallacious views for contrastive learning. Second, the level of perturbation is regarded as a very sensitive hyperparameter in such methods. Ablation studies in existing GCL literature [11, 13, 12] indicate that the performance of GCL models based on random augmentations are

*Corresponding author

Email addresses: h1ia0714@uni.sydney.edu.au (Huidong Liang), duxingjian.real@bytedance.com (Xingjian Du), zhubilei@bytedance.com (Bilei Zhu), mazejun@bytedance.com (Zejun Ma), knutchen@ucsd.edu (Ke Chen), junbin.gao@sydney.edu.au (Junbin Gao)

¹Both authors contributed equally.

²Work finished during an internship at ByteDance AI Lab.

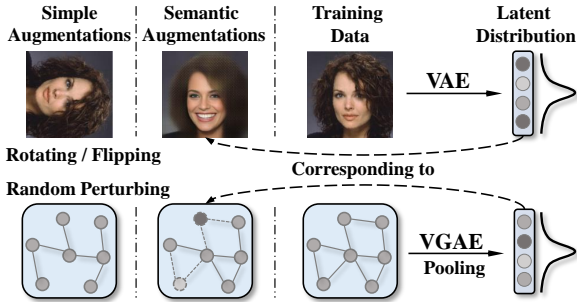


Figure 1: Illustration of simple augmentation and semantic augmentation in terms of image (top) and graph (bottom), where input data is sent to either VAE or VGAE to generate a latent distribution of low-dimensional vector that contains high-level meanings. Then the semantic augmentations of image or graph are performed by sampling from such distributions.

sensitive to the level of perturbation, where the optimal ratios often need to be tailored for different datasets after extensive hyper-parameter selection process. Therefore, to improve the effectiveness and efficiency in GCL, it is important to find an alternative way for graph data augmentation that can automatically generate different views and also retain graph semantics.

Meanwhile, implicit data augmentation methods [17, 18] have shown impressive results over the traditional augmentation methods in computer vision. Inspired by the high-level semantics preserved in deep neural networks’ embeddings [19], these approaches perform augmentation in the latent space rather than using simply flipped or rotated images as augmentations in the input space (illustrated in Figure 1), which provides a direction to improve the quality of augmentation in GCL. However, existing implicit augmentation methods are dependent on label information (i.e. supervised) and remain unexplored under graph settings. On the other hand, Variational Auto-Encoder (VAE) [20] is another powerful SSL model trained by reconstructing input features. Compared to simple image augmentation methods, embeddings sampled from the latent distributions in VAE correspond to high-level semantic meanings in the original image [21]. As demonstrated in Figure 1, semantic augmentations can be performed in the latent space of VAE or VGAE for different formats of data.

Despite of the reconstruction power of VAE and VGAE, the latent distributions often overlap with each other, making the embeddings difficult to separate for downstream tasks [22]. Therefore, we seek to address this overlapping issue by using graph contrastive method that aims to separate embeddings in the representation space, and in return, the semantic latent augmentations

from VGAE can further improve the effectiveness of GCL, leading to our innovations below.

Contributions

In this paper, we introduce *Implicit Graph Contrastive Learning* (iGCL) for both node-level and graph-level tasks, which exploits semantic latent augmentations from VGAE to improve the effectiveness of contrasting. To cohesively apply latent augmentation for contrastive learning, we propose a novel *Implicit Contrastive Loss* (ICL) with an upper bound for efficient training. Compared to the existing GCL methods based on augmentations with manual perturbations, our approach has the following contributions:

- iGCL exploits latent augmentations that preserves graph topological information, as opposed to classical GCL methods that create augmentations by randomly perturbing edges, nodes or attributes.
- The latent augmentations are learned automatically by reconstructing graph structure with a VGAE. Whereas the simple augmentations used in classical GCL methods are designed manually and often require tailored settings for different datasets.
- The proposed *Implicit Contrastive Loss*, unlike classical GCL methods that contrast two augmented views at each time, considers an expected loss w.r.t. all possible latent augmentations that contain graph structural information, and is optimized by an entropy-like upper-bound with a computational-efficient algorithm. This new loss objective is not limited to graph settings but can be applied to broader machine learning fields.

2. Related Work

2.1. Graph Contrastive Learning

Contrastive learning, an iconic self-supervised learning method that requires no label information for training, has received considerable attention in recent literature [23]. The general idea is to pull the positive views close in the representation space, and push the negative views apart via maximizing mutual information (MI). For example, Deep InfoMax [24] contrasts a global feature with other local features through a discriminator to maximize their MI; SimCLR [25] pulls augmentations generated from the same input together and push others apart with NT-Xent loss; CPC [26] contrasts the context point with other inputs to predict future inputs by optimizing the InfoNCE loss; and MoCo [27] further improves InfoNCE

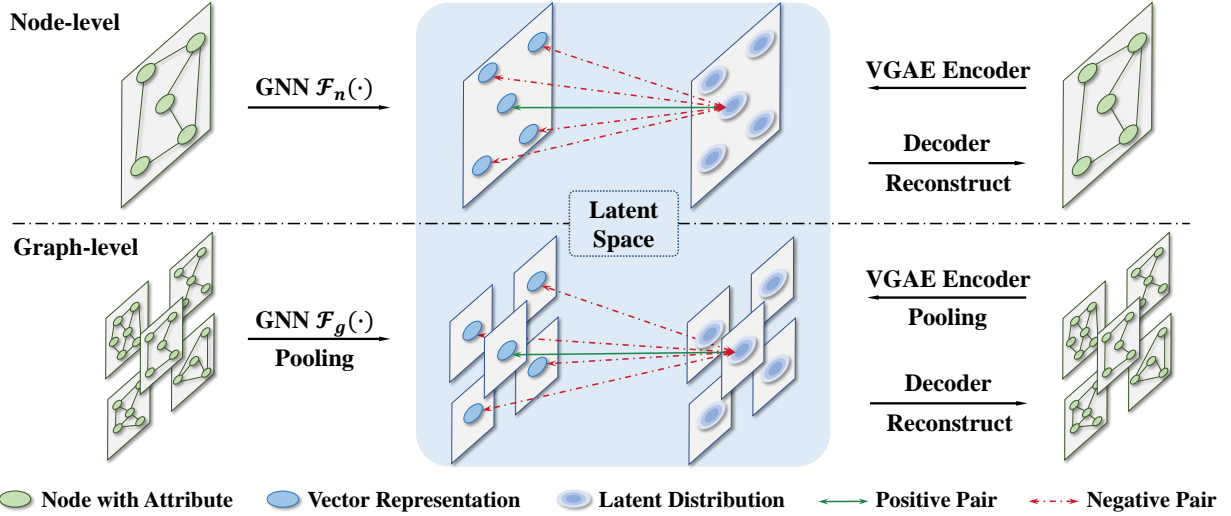


Figure 2: The overall structure of iGCL for node-level task (top) and graph-level task (bottom). For both tasks, we first use a GNN backbone to map the input graph (graphs) into vector representation for each node (graph), and at the same time, we obtain the latent distribution with identical dimension for each node (graph) by training an independent VGAE that reconstructs graph structure. Finally, graph contrastive learning is conducted in the latent space with the proposed *Implicit Contrastive Loss* and its upper bound in Eq.(13), where we regard the vector representation and the latent augmentation for the same node (graph) as positive pairs, and others as negative pairs, with details defined in section 3.2.2.

by applying momentum to the encoder that generates larger and more consistent dictionary. Currently, most of the graphs contrastive learning methods are extensions of the above works. At node-level, DGI [10] mimics Deep InfoMax by maximizing the MI of global representation and local representation; and GRACE [11] treats node representations of augmented views from the same node as positive pairs and others as negative pairs, then optimizes the model in a similar way to SimCLR. At graph-level, InfoGraph [14] extends DGI to graph-level tasks by maximizing the MI between graph-level and patch-level representations; and GraphCL [13] also adopts NT-Xent from SimCLR that treats augmentations for the same graph as positive pairs and others as negative pairs.

2.2. Graph Augmentation Methods

Similar to other fields, augmentation plays an important role in GCL. Common approaches include randomly adding or dropping node and edges [11, 13, 15], feature shuffling [10] and diffusion method [28]. However, random augmentations from these methods often change the graph structure and hence lead to meaningless graph views [16]. To address this issue, latest research begins to use adaptive augmentations such as GCA [12], or automated augmentation methods such as JOAO [29] and AutoGCL [30]. While these works utilize augmentations explicitly, our iGCL takes an implicit way to apply latent augmentations with graph semantic meanings. Unlike

existing latent augmentation methods in computer vision [17, 18], the proposed method generates latent augmentations in an unsupervised manner, and are optimized by a novel expected contrastive loss with a computationally efficient upper bound.

3. Methodology

Preliminaries

Let $\mathcal{G} = (\mathcal{V}, \mathcal{E})$ denote an undirected graph, where $\mathcal{V} = \{v_1, v_2, \dots, v_N\}$ and $\mathcal{E} \subseteq \mathcal{V} \times \mathcal{V}$ represent the node set and the edge set respectively. $\mathbf{X} \in \mathbb{R}^{N \times F}$ is the feature matrix for \mathcal{G} with rows $\{\mathbf{x}_1^\top, \mathbf{x}_2^\top, \dots, \mathbf{x}_N^\top\}$ (\mathbf{x}_i being a column-vector), and $\mathbf{A} \in \{0, 1\}^{N \times N}$ is the adjacency matrix with $A_{ij} = 1$ if $(v_i, v_j) \in \mathcal{E}$ and $A_{ij} = 0$ otherwise. Figure 2 demonstrates the overall structure of iGCL.

The following sections are organized to introduce the methodology of implicit augmentations on graph contrastive learning. In section 3.1, we demonstrate how we exploit the latent distributions from an independently-trained VGAE as the augmentation source for both node-level and graph-level tasks. In section 3.2.2, we introduce how we apply the novel *Implicit Contrastive Loss* to train a contrastive learning model by GNN backbones with latent augmentations. In section 3.3, we visualize the underlying rationale of iGCL and analyze its training object and broader impact.

3.1. Latent Augmentation with Graph Semantics

We aim to train a VGAE that reconstructs graph topological structure, and regard the latent distributions as the source for implicit contrastive learning in the next section. While the proposed algorithm is invariant to the choice of GNNs in VGAE, for simplicity, we adopt a standard 2-layer GCN as the encoder and assume the latent representation at the **final layer** $\mathbf{a}_n \in \mathbb{R}^D$ for node n follows a Gaussian distribution $\mathcal{N}(\boldsymbol{\mu}_n, \text{diag}(\boldsymbol{\sigma}_n^2))$, with $\boldsymbol{\mu}_n$ and $\boldsymbol{\sigma}_n$ parameterized by:

$$\mathbf{H}_\mu^{(\ell)} = \text{ReLU}(\tilde{\mathbf{D}}^{-\frac{1}{2}} \tilde{\mathbf{A}} \tilde{\mathbf{D}}^{-\frac{1}{2}} \mathbf{H}_\mu^{(\ell-1)}) \mathbf{W}_\mu^{(\ell)}, \quad (1)$$

$$\mathbf{H}_\sigma^{(\ell)} = \text{ReLU}(\tilde{\mathbf{D}}^{-\frac{1}{2}} \tilde{\mathbf{A}} \tilde{\mathbf{D}}^{-\frac{1}{2}} \mathbf{H}_\sigma^{(\ell-1)}) \mathbf{W}_\sigma^{(\ell)}, \quad (2)$$

where $\tilde{\mathbf{D}}_{ii} = \sum_j \tilde{\mathbf{A}}_{ij}$ is the degree matrix of $\tilde{\mathbf{A}}$ with $\tilde{\mathbf{A}} = \mathbf{A} + \mathbf{I}$. Both mean and variance encoding networks in Eq. (2) share the same weights in the first layer (i.e. $\mathbf{W}_\mu^{(0)} = \mathbf{W}_\sigma^{(0)}$) and use $\text{ReLU}(t) = \max(0, t)$ as the activation function. Note $\boldsymbol{\mu}_n^{(\ell)}$ and $\log \boldsymbol{\sigma}_n^{(\ell)}$ are both row-vectors in $\mathbf{H}_\mu^{(\ell)}$ and $\mathbf{H}_\sigma^{(\ell)}$ at the ℓ -th layer respectively, except for $\ell = 0$ where $\mathbf{H}_\sigma^{(0)} = \mathbf{H}_\mu^{(0)} = \mathbf{X}$.

The model is then optimized by maximizing the evidence lower bound \mathcal{L}_{VGAE} from variational inference:

$$\mathcal{L}_{VGAE} = \mathbb{E}_{q(\mathbf{H}|\mathbf{X}, \mathbf{A})} [\log p(\mathbf{A}|\mathbf{H})] - \text{KL}[q(\mathbf{H}|\mathbf{X}, \mathbf{A}) \| p(\mathbf{H})] \quad (3)$$

where the first term is the likelihood for reconstruction by an inner-product decoder $p(\mathbf{A}|\mathbf{H}) = \prod_{i=1}^N \prod_{j=1}^N \sigma(\mathbf{a}_i^\top \mathbf{a}_j)$ ($\sigma(\cdot)$ is the logistic sigmoid function). The second term regularizes the Kullback-Leibler divergence between the variational distribution $q(\mathbf{H}|\mathbf{X}, \mathbf{A}) = \prod_{n=1}^N q(\mathbf{a}_n|\mathbf{X}, \mathbf{A})$ (parameterized by the encoder networks) and a chosen prior $p(\mathbf{H}) = \prod_{n=1}^N p(\mathbf{a}_n) = \prod_{n=1}^N \mathcal{N}(\mathbf{a}_n|\mathbf{0}, \mathbf{I})$ (we adopt the standard Gaussian prior from the original paper). Upon convergence, we consider latent augmentations for node-level tasks and graph-level tasks separately below.

3.1.1. Latent Augmentation for Node-level Task

We define a latent augmentation $\tilde{\mathbf{a}}_n \in \mathbb{R}^D$ for node v_n as a sample from the learned latent distribution:

$$\tilde{\mathbf{a}}_n \sim \mathcal{N}(\boldsymbol{\mu}_n, \boldsymbol{\Sigma}_n), \quad (4)$$

where $\boldsymbol{\Sigma}_n$ is a diagonal matrix with elements in $\boldsymbol{\sigma}_n^2$. These augmentations contain topological information of the original graph: they can reconstruct the graph by a similarity matrix $\tilde{\mathbf{A}}$ of the original adjacency matrix \mathbf{A} by computing $\tilde{\mathbf{A}}_{ij} = \sigma(\tilde{\mathbf{a}}_i^\top \tilde{\mathbf{a}}_j)$.

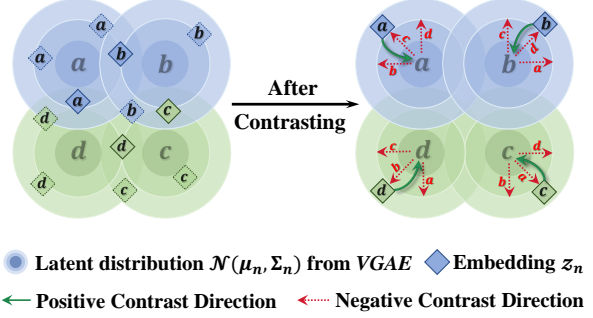


Figure 3: Illustration for the underlying behaviour of iGCL in Eq. (13). Suppose we generate latent distributions for nodes (graphs) a, b, c, d by VGAE and sample from them, the resulting embeddings (in dashed squares) could be hard to distinguish from their source distributions due to overlapping problem. However, after contrasting, embedding of node v_n (graph \mathcal{G}_n) is pushed away from the other nodes (graphs) distributions but also pulled close to its own distribution. Therefore, these new embeddings become more separated, and meanwhile preserve the graph structural information.

3.1.2. Latent Augmentation for Graph-level Task

Given a set of G graphs $\{\mathcal{G}_g\}_{g=1}^G$, we train a single VGAE on multiple graphs by reconstructing their graph structures, with training objective in Eq. (3) replaced by:

$$\mathcal{L}_{total} = \frac{1}{G} \sum_{g=1}^G \mathcal{L}_{VGAE}^{(g)}. \quad (5)$$

Then, we apply graph pooling in the embedding space to get a global representation \mathbf{r}_g for graph \mathcal{G}_g , which is also assumed to follow a Gaussian distribution $\mathcal{N}(\boldsymbol{\mu}_g, \text{diag}(\boldsymbol{\sigma}_g^2))$, with $\boldsymbol{\mu}_g$ and $\boldsymbol{\sigma}_g$ parameterized by a mean-aggregator used in [31, 32]:

$$\boldsymbol{\mu}_g = \frac{1}{N} \sum_{n=1}^N \boldsymbol{\mu}_n, \quad \log \boldsymbol{\sigma}_g = \frac{1}{N} \sum_{n=1}^N \log \boldsymbol{\sigma}_n, \quad (6)$$

where N is the number of nodes on graph \mathcal{G}_g and it can vary among different graphs. Similar to Eq. (4) for node-level augmentation, we can now define a latent augmentation $\tilde{\mathbf{r}}_g \in \mathbb{R}^D$ for graph \mathcal{G}_g as a sample from the latent distribution.

3.2. Implicit Graph Contrastive Learning

After obtaining the latent augmentations, at both node-level and graph-level, we train a GNN backbone by the proposed *Implicit Contrastive Loss* (ICL) below, with its underlying behaviour illustrated in Figure 3.

3.2.1. GNN Backbone

We consider two types of GNN backbones at node-level and graph-level: $\mathcal{F}_n(\mathbf{X}, \mathbf{A}) : \mathbb{R}^{N \times F} \times \mathbb{R}^{N \times N} \rightarrow \mathbb{R}^{N \times D}$

Algorithm 1 iGCL for Graph-level Task

Input: A set of graphs $\{\mathcal{G}_n\}_{n=1}^N$; Graph Auto-Encoder $VGAE(\cdot)$; GNN backbone $\mathcal{F}(\cdot)$ and projection head $\mathcal{P}(\cdot)$.

Parameter: Φ in $VGAE(\cdot)$; Θ in $\mathcal{F}(\cdot)$ and $\mathcal{P}(\cdot)$.

```
1: for  $epoch = 1, \dots, T$  do
2:   for  $batch$  in  $\{\mathcal{G}_n\}_{n=1}^N$  do
3:     Generate  $\mu_n, \sigma_n$  for  $\mathcal{G}_n$  from  $VGAE$  Eq. (6).
4:     for  $k = 1, \dots, K$  do
5:       Update  $\Phi$  by  $\nabla \mathcal{L}_{total}$  in Eq. (5).
6:     end for
7:     Generate  $z_n$  for graph  $\mathcal{G}_n$  from  $\mathcal{F}(\cdot)$  and  $\mathcal{P}(\cdot)$ .
8:     Update  $\Theta$  by  $\nabla \mathcal{L}_{upper}$  in Eq. (13).
9:   end for
10: end for
11: return Embedding  $\mathbf{Z}$  from the optimized  $\mathcal{F}(\cdot)$ .
```

that maps the input graph into N vector representations for node-level tasks, and $\mathcal{F}_g(\mathbf{X}, \mathbf{A}) : \mathbb{R}^{N \times F} \times \mathbb{R}^{N \times N} \rightarrow \mathbb{R}^D$ that maps the input graph into a global vector representation for graph-level tasks. Following the common choices in GCL literature, we adopt GCN or GAT as $\mathcal{F}_n(\cdot)$ and GIN [4] as $\mathcal{F}_g(\cdot)$. A non-linear projection head $\mathcal{P}(\cdot)$ (2-layer MLP) is also applied after the backbone to improve the expressive power [25]. Since both node-level and graph-level tasks aim to generate a vector representation for each node or for each graph respectively, for simplicity purpose, we will slightly abuse the notation z_n to represent the vector representation for node v_n in node-level tasks, or for graph \mathcal{G}_n in graph-level tasks for the rest of the paper.

3.2.2. Implicit Contrastive Loss

Following the *InfoNCE* [26] objective in contrastive learning, we sample M times from the latent distribution $\mathcal{N}(\mu_n, \Sigma_n)$ in Eq.(4), and denote \mathbf{a}_n^m as the m -th latent augmentation for node v_n in node-level tasks, or for graph \mathcal{G}_n in graph-level tasks. As demonstrated in Figure 2, for each augmentation sample, we regard (\mathbf{a}_n^m, z_n) as the positive pair, and $\{(\mathbf{a}_n^m, z_{n'})\}_{[n' \neq n]}$ as the negative pairs. Then the contrastive loss \mathcal{L}_{CL} for M augmentation samples is given by:

$$\mathcal{L}_{CL} = \frac{1}{N} \sum_{n=1}^N \frac{1}{M} \sum_{m=1}^M -\log \frac{\exp(z_n^\top \mathbf{a}_n^m / \tau)}{\sum_{n'=1}^N \exp(z_{n'}^\top \mathbf{a}_n^m / \tau)}, \quad (7)$$

where we use inner-product scaled by a temperature hyper-parameter τ as the similarity estimator.

Although a large M will improve the effectiveness of \mathcal{L}_{CL} , the algorithm becomes highly computational inefficient during optimization as the augmentation set is

Algorithm 2 iGCL for Node-level Task

Input: Graph \mathcal{G} with N nodes; Graph Auto-Encoder $VGAE(\cdot)$; GNN backbone $\mathcal{F}(\cdot)$ and projection head $\mathcal{P}(\cdot)$.

Parameter: Φ in $VGAE(\cdot)$; Θ in $\mathcal{F}(\cdot)$ and $\mathcal{P}(\cdot)$.

```
1: for  $epoch = 1, \dots, T$  do
2:   Generate  $\mu_n, \sigma_n$  for  $v_n$  from  $VGAE$ .
3:   for  $k = 1, \dots, K$  do
4:     Update  $\Phi$  by  $\nabla \mathcal{L}_{VGAE}$  in Eq. (3).
5:   end for
6:   Generate  $z_n$  for node  $v_n$  from  $\mathcal{F}(\cdot)$  and  $\mathcal{P}(\cdot)$ .
7:   Randomly sample a batch of size  $b$  from  $\{z_n\}_{n=1}^N$ .
8:   Compute  $\mathcal{L}_{upper}$  in Eq. (13) within the batch.
9:   Update  $\Theta$  by  $\nabla \mathcal{L}_{upper}$ .
10: end for
11: return Embedding  $\mathbf{Z}$  from the optimized  $\mathcal{F}(\cdot)$ .
```

enlarged by M times with a complexity of $O(MN^2D^2)$. To solve this problem, in the following section, we will investigate the situation when M grows to infinity, and propose an entropy-like upper bound that can be easily computed, hence leading to a more efficient algorithm.

Upper Bound

As $M \rightarrow \infty$, we are in fact discussing the expectation of the above contrastive loss for all possible latent augmentations, which is defined as the *Implicit Contrastive Loss* $\mathcal{L}_{ICL} := \lim_{M \rightarrow +\infty} \mathcal{L}_{CL}$ as follows:

$$\mathcal{L}_{ICL} = \frac{1}{N} \sum_{n=1}^N \mathbb{E}_{\tilde{\mathbf{a}}_n} \left[-\log \frac{\exp(z_n^\top \tilde{\mathbf{a}}_n / \tau)}{\sum_{n'=1}^N \exp(z_{n'}^\top \tilde{\mathbf{a}}_n / \tau)} \right] \quad (8)$$

$$= \frac{1}{N} \sum_{n=1}^N \mathbb{E}_{\tilde{\mathbf{a}}_n} \left[\log \sum_{n'=1}^N \exp((z_{n'} - z_n)^\top \tilde{\mathbf{a}}_n / \tau) \right]. \quad (9)$$

Given the Jensen's inequality $\mathbb{E}[\log X] \leq \log \mathbb{E}[X]$, we can find an upper bound \mathcal{L}_{upper} for \mathcal{L}_{ICL} by swapping the log and expectation, that is, $\mathcal{L}_{upper} \geq \mathcal{L}_{ICL}$ with:

$$\mathcal{L}_{upper} = \frac{1}{N} \sum_{n=1}^N \log \mathbb{E}_{\tilde{\mathbf{a}}_n} \left[\sum_{n'=1}^N \exp((z_{n'} - z_n)^\top \tilde{\mathbf{a}}_n / \tau) \right]. \quad (10)$$

Since $\delta_{n'n} := z_{n'} - z_n$ is a constant inside the expectation in Eq.(10) and $\tilde{\mathbf{a}}_n$ follows $\mathcal{N}(\mu_n, \Sigma_n)$, we can rewrite \mathcal{L}_{upper} with the moment generating function:

$$\mathbb{E}[\exp(tX)] = \exp(t\mu + \frac{1}{2}\sigma^2 t^2), \quad X \sim \mathcal{N}(\mu, \sigma^2), \quad (11)$$

which transforms the expectation form of \mathcal{L}_{upper} into:

$$\frac{1}{N} \sum_{n=1}^N \log \sum_{n'=1}^N \exp(\delta_{n'n}^\top \mu_n / \tau + \delta_{n'n}^\top \Sigma_n \delta_{n'n} / 2\tau^2). \quad (12)$$

Graph	Dataset	MUTAG	NCI1	PROTEINS	COLLAB	IMDB-B	IMDB-M
Statistics	Type	Molecule	Molecule	Molecule	Social	Social	Social
	# Graphs	188	4,110	1,113	5,000	1,000	1,500
	# Classes	2	2	2	3	2	3
	Avg. Nodes	17.9	29.9	39.1	74.5	19.8	13.0
	Avg. Edges	19.8	32.3	72.8	2,457.8	96.5	65.9
Settings	Projection	Skip	Linear	Linear	Linear	Linear	Skip
	num_epochs	100	100	20	20	20	100
	num_layers	5	5	2	8	2	8
	emb_size	256	256	256	256	512	128
	batch_size	16	32	64	128	16	64
	lr	5×10^{-4}	10^{-4}	10^{-4}	5×10^{-4}	10^{-4}	5×10^{-4}
	ℓ_2	5×10^{-3}	5×10^{-3}	10^{-2}	10^{-2}	5×10^{-3}	10^{-2}
	τ	0.01	3.54	5	1.98	5.0	10.0

Table 1: Dataset statistics and hyper-parameter settings for Graph-level tasks.

Finally, we restore Eq.(12) to an entropy-like equivalent:

$$\frac{1}{N} \sum_{n=1}^N -\log \frac{\exp(\mathbf{z}_n^\top \boldsymbol{\mu}_n / \tau)}{\sum_{n'=1}^N \exp(\mathbf{z}_{n'}^\top \boldsymbol{\mu}_n / \tau + \boldsymbol{\sigma}_n \odot \boldsymbol{\delta}_{n'n}^\top \boldsymbol{\delta}_{n'n} / 2\tau^2)} \quad (13)$$

where we further simplify the quadratic term $\boldsymbol{\delta}_{n'n}^\top \boldsymbol{\Sigma}_n \boldsymbol{\delta}_{n'n}$ into an element-wise operation $\boldsymbol{\sigma}_n \odot \boldsymbol{\delta}_{n'n}^\top \boldsymbol{\delta}_{n'n}$, since $\boldsymbol{\Sigma}_n$ is a diagonal matrix with diagonal entries $\boldsymbol{\sigma}_n$. Compared to \mathcal{L}_{CL} in Eq. (7), the proposed upper bound in Eq. (13) is more efficient with a complexity of $\mathcal{O}(N^2 D^2)$. We demonstrate the learning algorithms for iGCL at graph-level and node-level in Algorithm 1 and Algorithm 2.

3.3. Interpretation of iGCL and Broader Impact

We present a visual explanation shown in Figure 3 to explain the underlying behaviour of applying implicit contrastive loss ICL in Eq. (13). The objective of iGCL is to contrast on the latent distributions from VGAE, where embedding \mathbf{z}_n for node v_n (graph \mathcal{G}_n) are pushed away from the means of the other nodes’ latent distributions, and pulled close to the mean of its own latent distribution, with temperature τ controlling the contrastive scale such that it won’t be excessively far away for reconstruction. In this way, ICL enables a GNN backbone $\mathcal{F}(\cdot)$ to separate the embeddings of different nodes (or graphs) and maintain graph semantic information at the same time. Moreover, compared to existing GCL methods such as GraphCL (from SimCLR) and InfoGraph (from Deep InfoMax) that only contrast two augmented views at each training epoch, iGCL contrast with the distributions of all possible latent augmentations at each iteration but requires the same level of complexity, credited to the computational-efficient upper bound.

The proposed *Implicit Contrastive Learning* approach does not only limit to graph settings and can be extended to other machine learning fields. The general idea is to first train a VAE that can generate high-level latent distributions with semantic meanings, then regard them as the source for latent augmentations and conduct implicit contrastive learning with the proposed upper bound for ICL in Eq. (13). To the best of our knowledge, no similar approach has been explored in the existing literature.

4. Experiment

In this section, we empirically evaluate our proposed method on graph-level and node-level tasks, and compare the performance with other state-of-the-art GNN methods. An ablation study is also conducted in the end to discuss the effectiveness of different modules in our model. Code for reproducing the experiment results can be found in the supplementary materials.

4.1. Graph-level Tasks

4.1.1. Settings

For graph-level tasks, we test our model by classification task on three biochemical molecule networks: MUTAG [33], NCI1[34] and PROTEINS [35]; and three social networks: COLLAB [36], IMDB-B and IMDB-M [37], where detailed dataset statistics are summarized in Table 1. The selected baselines for comparison are three classic unsupervised methods: node2vec [38], sub2vec [39] and graph2vec [40]; two common GCL baselines: InfoGraph [14] and GraphCL[13]; and two latest GCL methods with automated augmentations: JOAO [29] and AutoGCL [30]. The experiment results for these baselines are adopted from their original papers or reproduced by the official codes released from their authors.

Input	Method	MUTAG	NCI1	PROTEINS	COLLAB	IMDB-B	IMDB-M
A, X, Y	GCN	85.6 ± 5.8	80.2 ± 2.0	74.9 ± 3.3	79.0 ± 1.8	70.4 ± 3.4	51.9 ± 3.8
	GIN	89.4 ± 5.6	82.7 ± 1.7	76.2 ± 2.8	80.2 ± 1.9	75.1 ± 5.1	52.3 ± 2.8
A, X	node2vec	72.6 ± 10.2	54.9 ± 1.6	57.5 ± 3.6	56.1 ± 0.2	50.2 ± 0.9	36.0 ± 0.7
	sub2vec	61.1 ± 15.9	52.8 ± 1.5	53.0 ± 5.6	-	55.3 ± 1.5	36.7 ± 0.8
	graph2vec	83.2 ± 9.3	73.2 ± 1.8	73.3 ± 2.1	-	71.1 ± 0.5	50.4 ± 0.9
	InfoGraph	89.0 ± 1.1	76.2 ± 1.0	74.4 ± 0.3	70.7 ± 1.1	73.0 ± 0.9	49.7 ± 0.5
	GraphCL	86.8 ± 1.3	77.9 ± 0.4	74.4 ± 0.5	71.4 ± 1.1	71.1 ± 0.4	49.2 ± 0.6
	JOAO	87.4 ± 1.0	78.1 ± 0.5	74.6 ± 0.4	69.5 ± 0.4	70.2 ± 3.1	-
	AutoGCL	88.6 ± 1.1	82.0 ± 0.3	75.8 ± 0.4	70.1 ± 0.7	73.3 ± 0.4	-
	iGCL (ours)	89.8 ± 1.2	82.7 ± 0.4	74.8 ± 0.5	72.0 ± 0.8	72.6 ± 0.6	49.8 ± 0.6

Table 2: Graph Classification Results. Numbers highlighted in **bold** and **blue** represent the **best** and the **second** best results respectively.

4.1.2. Graph Classification

We closely follow the common approach in GCL for graph classification [14, 13]: the GNN backbone is chosen as GIN [4] with layers from {2,5,8} and embedding size from {128, 256, 512}. After contrastive learning, we use a SVM as the classifier with hyper-parameter C chosen from $\{10^{-3}, 10^{-2}, \dots, 10^2, 10^3\}$ and report the 10-fold cross validation accuracy as the final result. The experiments are repeated 10 times for graph classification, with evaluation accuracy reported by mean and standard deviation. Detailed hyper-parameter settings for reproduction are summarized in Table 1.

The results in Table 2 indicate that iGCL outperforms classic GCL baselines InfoGraph and GraphCL on five datasets and achieves comparable result on IMDB-B. Compared with JOAO and AutoGCL that use automated augmentation method in GCL, iGCL also shows the best performance on MUTAG, NCI1 and COLLAB, and ranks the second best on PROTEINS and IMDB-M.

4.2. Node-level Tasks

4.2.1. Settings

In this section, we validate iGCL on node-level classification and clustering tasks. The datasets used for evaluation are three citation networks: Cora, Citeseer and PubMed [41]; and two Amazon sales dataset: Computers and Photo [42], where the statistics are summarized in Table 3. For node classification tasks, We compare our model against two GCL methods with random augmentations: DGI [10] and GRACE [11]; a non-augmentation method GMI [43]; and an adaptive augmentation method GCA [12]. For node clustering, we compare iGCL to three classical clustering methods on graphs: K-means, Spectral Clustering [44] and DeepWalk [45]; three Graph

Auto-Encoder models: VGAE [46], ARGAE [47] and GALA [48], plus a contrastive method MVGRL [28]. The results are retained from original papers or reproduced by the official codes from their authors.

4.2.2. Node Classification

For node classification task, we adopt the standard dataset splits for citation networks [1] and Amazon sales [12]. We follow the common search strategy [11, 12] in GCL for our model configurations: the GNN backbone is selected as GCN [1] or GAT [2] with layers from 1, 2, 3 and embedding sizes from 128, 256, 512, and the projection function is chosen as a 2-layer MLP. After unsupervised training, a logistic regression classifier is applied to the learned embeddings for the downstream node classification task, where the final testing accuracy is selected at the epoch with the best validation accuracy. Experiments are repeated 20 times with accuracy reported by mean and standard deviation in Table 4. Detailed model settings are summarized in Table 3.

The results show that, except for Citeseer, iGCL outperforms classical node-level GCL methods DGI, GMI and GRACE on the rest five datasets. Compared to GCA that uses adaptive augmentation, iGCL performs better on Cora and Computers, and comparably on PubMed with a slight disadvantage.

4.2.3. Node Clustering

After contrastive training, we perform clustering on the learned embeddings using K-means algorithm, where three metrics are used for evaluation: accuracy (Acc), normalized mutual information (NMI) and adjusted random index (ARI), with results presented in Table 5. We can see that iGCL achieves comparable results with other

Node	Dataset	Cora	Citeseer	PubMed	Photo	Computers
Statistics	Type	Citation	Citation	Citation	Amazon Sales	Amazon Sales
	# Features	1,433	3,703	500	745	767
	# Classes	7	6	3	8	10
	# Nodes	2,708	3,327	19,717	7,650	13,752
	# Edges	5,429	4,732	44,338	119,081	245,861
Settings	Backbone	GCN	GAT	GCN	GAT	GAT
	num_epochs	300	300	1000	600	600
	emb_size	256	512	128	256	256
	dropout	0.5	0.5	0.5	0.5	0.5
	lr	10^{-4}	5×10^{-4}	10^{-4}	5×10^{-3}	10^{-3}
	lr step	-	0.85	-	0.85	0.85
	ℓ_2	5×10^{-3}	10^{-2}	10^{-4}	5×10^{-3}	5×10^{-3}
τ	1.0	5.0	4.7	1.0	1.0	

Table 3: Dataset statistics and hyper-parameter settings for Node-level task.

Input	Method	Cora	Citeseer	PubMed	Photo	Computers
A, X, Y	GCN	81.5 \pm 0.2	70.3 \pm 0.4	79.0 \pm 0.5	92.4 \pm 0.2	86.5 \pm 0.5
	GraphSAGE	83.0 \pm 0.7	72.5 \pm 0.7	79.0 \pm 0.3	92.6 \pm 0.4	86.9 \pm 0.3
	GAT	83.0 \pm 0.7	72.5 \pm 0.7	79.0 \pm 0.3	92.6 \pm 0.4	86.9 \pm 0.3
A, X	GAE	74.9 \pm 0.4	65.6 \pm 0.5	74.2 \pm 0.3	91.6 \pm 0.1	85.3 \pm 0.2
	VGAE	76.3 \pm 0.2	66.8 \pm 0.2	75.8 \pm 0.4	92.2 \pm 0.1	86.4 \pm 0.2
	DGI	82.3 \pm 0.6	71.8 \pm 0.7	76.8 \pm 0.6	91.6 \pm 0.2	84.0 \pm 0.5
	GMI	83.0 \pm 0.3	73.0 \pm 0.3	80.1 \pm 0.2	90.7 \pm 0.2	82.2 \pm 0.3
	GRACE	83.3 \pm 0.4	72.1 \pm 0.5	80.6 \pm 0.4	91.5 \pm 0.4	87.1 \pm 0.3
	GCA	83.1 \pm 0.3	72.3 \pm 0.5	80.9 \pm 0.3	92.5 \pm 0.2	87.8 \pm 0.3
	iGCL (ours)	83.6 \pm 0.6	72.2 \pm 0.6	80.8 \pm 0.6	92.5 \pm 0.5	88.1 \pm 0.3

Table 4: Node Classification Results. Numbers highlighted in **bold** and **blue** represent the **best** and the **second** best results respectively.

Input	Method	Cora			Citeseer			PubMed		
		Acc	NMI	ARI	Acc	NMI	ARI	Acc	NMI	ARI
A	K-means	0.492	0.321	0.230	0.540	0.305	0.279	0.398	0.001	0.002
	SC	0.367	0.127	0.031	0.239	0.056	0.010	0.403	0.042	0.002
	DeepWalk	0.484	0.327	0.243	0.337	0.088	0.092	0.684	0.279	0.299
A, X	GAE	0.596	0.429	0.347	0.408	0.176	0.124	0.672	0.277	0.279
	VGAE	0.443	0.239	0.175	0.344	0.156	0.093	0.630	0.229	0.213
	ARGA	0.640	0.449	0.352	0.573	0.350	0.341	0.668	0.305	0.295
	ARVGA	0.638	0.450	0.374	0.544	0.261	0.245	0.690	0.290	0.306
	GALA	0.746	0.577	0.532	0.693	0.441	0.446	0.694	0.327	0.321
	MVGRL	0.732	0.569	0.522	0.691	0.437	0.449	0.687	0.319	0.315
	iGCL	0.744	0.566	0.539	0.695	0.435	0.452	0.697	0.334	0.329

Table 5: Node Clustering Results. Numbers highlighted in **bold** and **blue** represent the **best** and the **second** best results respectively.

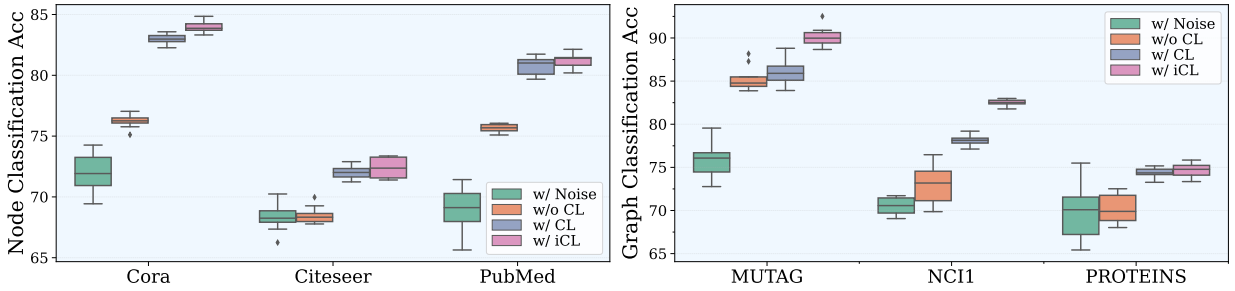


Figure 4: The ablation study of training with different modules at both node-level (left) and graph-level (right).

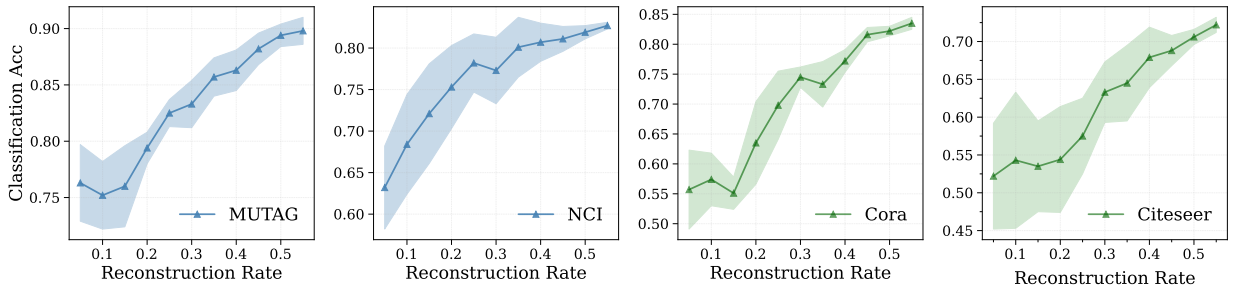


Figure 5: The sensitivity of graph (left two plots in blue) and node (right two plots in green) classification accuracy to reconstruction accuracy. Triangle represents the mean accuracy and shaded area represents the interval within one standard deviation.

state-of-the-art models on Cora and Citeseer datasets, meanwhile slightly outperforms the other baselines on PubMed under all metrics.

4.3. Ablation Studies

We investigate three cases to demonstrate the advantages of adopting implicit augmentations for graph contrastive learning: 1) Comparison between different training strategies; 2) the sensitivity of the downstream classification performance to VGAE reconstruction rate; and 3) the visual comparison of the embeddings learned from VGAE and our iGCL.

4.3.1. Effectiveness of Different Modules

We compare four different training strategies on both node-level and graph-level tasks: (a) contrasting with random Gaussian Noise, that is, fixing $\mu = \mathbf{0}$ and $\Sigma = \mathbf{I}$ in Eq. (13) (denoted as w/ Noise), (b) using VGAE embeddings without contrastive learning (w/o CL), (c) using standard graph contrastive learning approach in Eq.(7), where we substitute \mathbf{a}_n^m with embeddings generated by the same GNN backbone using augmented graph views based on node and edge perturbation (w/ CL), and (d) using full iGCL model (w/ iCL). The experiments are repeated 10 times with results summarized in Figure 4.

The box plots manifest that by adopting implicit augmentations, iGCL consistently outperforms classical contrastive methods on five datasets except for Citeseer, where iGCL underperforms by a small margin. Interestingly, contrasting with a standard normal distribution $\mathcal{N}(\mathbf{0}, \mathbf{I})$ can achieve around 70% classification accuracy on all six datasets, which is comparable to VGAE on Citeseer, NCI1 and PROTEINS. We attribute this phenomenon to the standard normal prior choice in VGAE, as \mathcal{L}_{VGAE} in Eq. 3 regularizes the latent distributions to the prior.

4.3.2. Sensitivity to Reconstruction Accuracy

In this section, we analyze the sensitivity of iGCL’s performance regarding to the reconstruction accuracy of VGAE. We first train an independent VGAE and stop the training process when reconstruction rate is at around 10%,20%,...,60%, then use the learned latent distributions (μ and σ) as the source for latent augmentations in iGCL, and finally evaluate the classification accuracy based on the learned embeddings at each reconstruction rate. We repeat the experiment 10 times and illustrate the results in Figure 5. We can see that at both graph-level and node-level, there is a positive correlation between the reconstruction rate and final classification accuracy, which corroborates the claim that latent augmentations

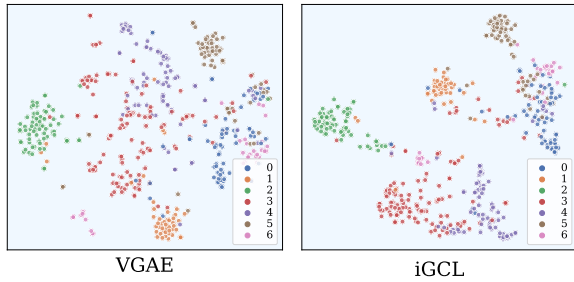


Figure 6: Embedding visualizations from VGAE (left) and iGCL (right) on Cora dataset using t-SNE, where colours represent node labels.

with better quality can improve the contrastive learning performance on downstream tasks.

4.3.3. Visual Comparison with VGAE embeddings

To visualize the training results, we project the embeddings from VGAE and our iGCL into 2-dimensional space using t-SNE algorithm [49] under the same settings on Cora dataset (50 perplexity with 1000 iterations), and present the embedding visualization in Figure 6. While both methods can generate embeddings that are separable at some level, we can observe that nodes with red (3), purple (4) and blue (0) labels are more tightly clustered by iGCL as opposed to the results from VGAE, indicating the advantage of adopting implicit contrastive learning for downstream tasks.

5. Conclusion

In this paper we introduce *Implicit Graph Contrastive Learning* (iGCL), an algorithm that exploits semantic augmentations in the latent space learned from a VGAE by reconstructing graph topological structure. The proposed method adopts an *Implicit Contrastive Loss* that considers the expected contrastive loss w.r.t. all possible latent augmentations and is optimized by an entropy-like upper bound to improve computational efficiency. Experiments on both node-level and graph-level tasks indicate that iGCL achieves state-of-the-art performances compared to other GCL methods. Lastly, the ablation studies demonstrate the effectiveness of implicit contrastive learning and latent augmentation, which have potential extension to other machine learning domains.

References

[1] T. N. Kipf, M. Welling, Semi-supervised classification with graph convolutional networks, in: International Conference on Learning Representations, 2017.

[2] P. Veličković, G. Cucurull, A. Casanova, A. Romero, P. Lio, Y. Bengio, Graph attention networks, in: International Conference on Learning Representations, 2018.

[3] W. L. Hamilton, R. Ying, J. Leskovec, Inductive representation learning on large graphs, in: Proceedings of the 31st International Conference on Neural Information Processing Systems, 2017, pp. 1025–1035.

[4] K. Xu, W. Hu, J. Leskovec, S. Jegelka, How powerful are graph neural networks?, in: International Conference on Learning Representations, 2019.

[5] P. Xu, W. Hu, J. Wu, B. Du, Link prediction with signed latent factors in signed social networks, in: Proceedings of the 25th ACM SIGKDD International Conference on Knowledge Discovery and Data Mining, 2019, pp. 1046–1054.

[6] J. Gasteiger, F. Becker, S. Günnemann, Gemnet: Universal directional graph neural networks for molecules, Advances in Neural Information Processing Systems 34 (2021) 6790–6802.

[7] R. Ying, R. He, K. Chen, P. Eksombatchai, W. L. Hamilton, J. Leskovec, Graph convolutional neural networks for web-scale recommender systems, in: Proceedings of the 24th ACM SIGKDD international conference on knowledge discovery & data mining, 2018, pp. 974–983.

[8] Y. Liu, M. Jin, S. Pan, C. Zhou, Y. Zheng, F. Xia, P. Yu, Graph self-supervised learning: A survey, IEEE Transactions on Knowledge and Data Engineering (2022).

[9] Y. Xie, Z. Xu, J. Zhang, Z. Wang, S. Ji, Self-supervised learning of graph neural networks: A unified review, IEEE Transactions on Pattern Analysis and Machine Intelligence (2022).

[10] P. Veličković, W. Fedus, W. L. Hamilton, P. Liò, Y. Bengio, R. D. Hjelm, Deep graph infomax, in: International Conference on Learning Representations, 2019.

[11] Y. Zhu, Y. Xu, F. Yu, Q. Liu, S. Wu, L. Wang, Deep graph contrastive representation learning, arXiv preprint arXiv:2006.04131 (2020).

[12] Y. Zhu, Y. Xu, F. Yu, Q. Liu, S. Wu, L. Wang, Graph contrastive learning with adaptive augmentation, in: Proceedings of the Web Conference 2021, 2021, pp. 2069–2080.

[13] Y. You, T. Chen, Y. Sui, T. Chen, Z. Wang, Y. Shen, Graph contrastive learning with augmentations, Advances in Neural Information Processing Systems 33 (2020) 5812–5823.

[14] F.-Y. Sun, J. Hoffman, V. Verma, J. Tang, Infograph: Unsupervised and semi-supervised graph-level representation learning via mutual information maximization, in: International Conference on Learning Representations, 2020.

[15] D. Xu, W. Cheng, D. Luo, H. Chen, X. Zhang, Infogcl: Information-aware graph contrastive learning, Advances in Neural Information Processing Systems 34 (2021) 30414–30425.

[16] N. Lee, J. Lee, C. Park, Augmentation-free self-supervised learning on graphs, in: Proceedings of the AAAI Conference on Artificial Intelligence, Vol. 36, 2022, pp. 7372–7380.

[17] Y. Wang, X. Pan, S. Song, H. Zhang, G. Huang, C. Wu, Implicit semantic data augmentation for deep networks, Advances in Neural Information Processing Systems 32 (2019).

[18] S. Li, K. Gong, C. H. Liu, Y. Wang, F. Qiao, X. Cheng, Metasaug:

- Meta semantic augmentation for long-tailed visual recognition, in: Proceedings of the IEEE/CVF conference on computer vision and pattern recognition, 2021, pp. 5212–5221.
- [19] Y. LeCun, Y. Bengio, G. Hinton, Deep learning, *nature* 521 (7553) (2015) 436–444.
- [20] D. P. Kingma, M. Welling, Auto-encoding variational Bayes, in: International Conference on Learning Representations, 2014.
- [21] W. Liu, R. Li, M. Zheng, S. Karanam, Z. Wu, B. Bhanu, R. J. Radke, O. Camps, Towards visually explaining variational autoencoders, in: Proceedings of the IEEE/CVF Conference on Computer Vision and Pattern Recognition, 2020.
- [22] E. Mathieu, T. Rainforth, N. Siddharth, Y. W. Teh, Disentangling disentanglement in variational autoencoders, in: International Conference on Machine Learning, PMLR, 2019, pp. 4402–4412.
- [23] X. Liu, F. Zhang, Z. Hou, L. Mian, Z. Wang, J. Zhang, J. Tang, Self-supervised learning: Generative or contrastive, *IEEE Transactions on Knowledge and Data Engineering* (2021).
- [24] R. D. Hjelm, A. Fedorov, S. Lavoie-Marchildon, K. Grewal, P. Bachman, A. Trischler, Y. Bengio, Learning deep representations by mutual information estimation and maximization, in: International Conference on Learning Representations, 2018.
- [25] T. Chen, S. Kornblith, M. Norouzi, G. Hinton, A simple framework for contrastive learning of visual representations, in: International conference on machine learning, PMLR, 2020, pp. 1597–1607.
- [26] A. v. d. Oord, Y. Li, O. Vinyals, Representation learning with contrastive predictive coding, *arXiv preprint arXiv:1807.03748* (2018).
- [27] K. He, H. Fan, Y. Wu, S. Xie, R. Girshick, Momentum contrast for unsupervised visual representation learning, in: Proceedings of the IEEE/CVF conference on computer vision and pattern recognition, 2020, pp. 9729–9738.
- [28] K. Hassani, A. H. Khasahmadi, Contrastive multi-view representation learning on graphs, in: International Conference on Machine Learning, PMLR, 2020, pp. 4116–4126.
- [29] Y. You, T. Chen, Y. Shen, Z. Wang, Graph contrastive learning automated, in: International Conference on Machine Learning, PMLR, 2021, pp. 12121–12132.
- [30] Y. Yin, Q. Wang, S. Huang, H. Xiong, X. Zhang, Autogl: Automated graph contrastive learning via learnable view generators, in: Proceedings of the AAAI Conference on Artificial Intelligence, Vol. 36, 2022, pp. 8892–8900.
- [31] M. Garnelo, D. Rosenbaum, C. Maddison, T. Ramalho, D. Saxton, M. Shanahan, Y. W. Teh, D. Rezende, S. A. Eslami, Conditional neural processes, in: International Conference on Machine Learning, PMLR, 2018, pp. 1704–1713.
- [32] M. Garnelo, J. Schwarz, D. Rosenbaum, F. Viola, D. J. Rezende, S. Eslami, Y. W. Teh, Neural processes, *arXiv:1807.01622* (2018).
- [33] A. K. Debnath, R. L. Lopez de Compadre, G. Debnath, A. J. Shusterman, C. Hansch, Structure-activity relationship of mutagenic aromatic and heteroaromatic nitro compounds. correlation with molecular orbital energies and hydrophobicity, *Journal of medicinal chemistry* 34 (2) (1991) 786–797.
- [34] N. Wale, I. A. Watson, G. Karypis, Comparison of descriptor spaces for chemical compound retrieval and classification, *Knowledge and Information Systems* 14 (3) (2008) 347–375.
- [35] K. M. Borgwardt, C. S. Ong, S. Schönauer, S. Vishwanathan, A. J. Smola, H.-P. Kriegel, Protein function prediction via graph kernels, *Bioinformatics* 21 (suppl_1) (2005) i47–i56.
- [36] J. Leskovec, J. Kleinberg, C. Faloutsos, Graphs over time: densification laws, shrinking diameters and possible explanations, in: Proceedings of the eleventh ACM SIGKDD international conference on Knowledge discovery in data mining, 2005, pp. 177–187.
- [37] P. Yanardag, S. Vishwanathan, Deep graph kernels, in: Proceedings of the 21th ACM SIGKDD international conference on knowledge discovery and data mining, 2015, pp. 1365–1374.
- [38] A. Grover, J. Leskovec, node2vec: Scalable feature learning for networks, in: Proceedings of the 22nd ACM SIGKDD International Conference on Knowledge Discovery and Data Mining, 2016, pp. 855–864.
- [39] B. Adhikari, Y. Zhang, N. Ramakrishnan, B. A. Prakash, Sub2vec: Feature learning for subgraphs, in: Pacific-Asia Conference on Knowledge Discovery and Data Mining, Springer, 2018, pp. 170–182.
- [40] A. Narayanan, M. Chandramohan, R. Venkatesan, L. Chen, Y. Liu, S. Jaiswal, graph2vec: Learning distributed representations of graphs, *arXiv preprint arXiv:1707.05005* (2017).
- [41] P. Sen, G. Namata, M. Bilgic, L. Getoor, B. Galligher, T. Eliassi-Rad, Collective classification in network data, *AI magazine* 29 (3) (2008) 93–93.
- [42] J. McAuley, C. Targett, Q. Shi, A. Van Den Hengel, Image-based recommendations on styles and substitutes, in: Proceedings of the 38th international ACM SIGIR conference on research and development in information retrieval, 2015, pp. 43–52.
- [43] Z. Peng, W. Huang, M. Luo, Q. Zheng, Y. Rong, T. Xu, J. Huang, Graph representation learning via graphical mutual information maximization, in: Proceedings of The Web Conference, 2020, pp. 259–270.
- [44] L. Tang, H. Liu, Leveraging social media networks for classification, *Data Mining and Knowledge Discovery* 23 (3) (2011) 447–478.
- [45] B. Perozzi, R. Al-Rfou, S. Skiena, Deepwalk: Online learning of social representations, in: Proceedings of the 20th ACM SIGKDD International Conference on Knowledge Discovery and Data Mining, 2014, pp. 701–710.
- [46] T. N. Kipf, M. Welling, Variational graph auto-encoders, *arXiv:1611.07308* (2016).
- [47] S. Pan, R. Hu, G. Long, J. Jiang, L. Yao, C. Zhang, Adversarially regularized graph autoencoder for graph embedding, in: International Joint Conference on Artificial Intelligence, 2018.
- [48] J. Park, M. Lee, H. J. Chang, K. Lee, J. Y. Choi, Symmetric graph convolutional autoencoder for unsupervised graph representation learning, in: Proceedings of the IEEE/CVF International Conference on Computer Vision, 2019, pp. 6519–6528.
- [49] L. Van der Maaten, G. Hinton, Visualizing data using t-sne, *Journal of Machine Learning Research* 9 (11) (2008).